

Anomalous self-similarity in a turbulent rapidly rotating fluid

Charles N. Baroud¹, Brendan B. Plapp¹, Zhen-Su She^{2,3}, and Harry L. Swinney¹

¹*Center for Nonlinear Dynamics and Department of Physics, The University of Texas at Austin, Austin, TX 78712*

²*State Key Laboratory for Turbulence Research, Department of Mechanics and Engineering Science, Peking University, Beijing 100871, China*

³*Department of Mathematics, UCLA, Los Angeles, CA 90095*

(November 4, 2018)

Abstract

Our velocity measurements on the quasi-two-dimensional turbulent flow in a rapidly rotating annulus yield an inverse energy cascade with $E(k) \sim k^{-2}$ rather than the expected $E(k) \sim k^{-5/3}$. The probability distribution functions for longitudinal velocity differences, $\delta v(\ell) = v(x + \ell) - v(x)$, are self-similar (scale independent) but strongly non-Gaussian, which suggests that the coherent vortices play a significant role. The structure functions, $\langle [\delta v(\ell)]^p \rangle \sim \ell^{\zeta_p}$, exhibit anomalous scaling: $\zeta_p = \frac{p}{2}$ rather than the expected $\zeta_p = \frac{p}{3}$.

PACS: 47.27.-i, 92.10.Lq, 47.32.Cc

In large scale flows in the earth's atmosphere and oceans or in gaseous planets, the Coriolis force dominates other forces and to lowest order is balanced by pressure gradients (geostrophic balance). The dimensionless number that characterizes this regime is the Rossby number, the ratio of magnitudes of the inertial term in the Navier-Stokes equation ($\vec{u} \cdot \nabla \vec{u}$, where \vec{u} is the velocity) to the Coriolis term ($2\vec{\Omega} \times \vec{u}$, where Ω is the rotation rate). For planetary flows on large scales the Rossby number is typically in the range 0.05-2, and turbulence in such flows is quite different from three-dimensional (3D) turbulence in an inertial reference frame. Despite the importance of planetary flows, geostrophic turbulence has scarcely been examined in laboratory experiments. Our experiments in a rotating annulus are the first to determine the scaling properties of turbulence in a low Rossby number flow.

One of the most significant effects of rapid rotation on a fluid is the two-dimensionalization of the flow [1]. Recent numerical simulations of a rotating turbulent flow recovered quasi-2-dimensionality even in the case of 3D forcing [2]. Turbulence in a 2D rapidly rotating flow has some similarities to other 2D turbulent flows, but the rapid rotation leads to the formation of large vortices and jets, hence a flow that is more inhomogeneous and anisotropic [1].

The statistics of velocity differences for 2D turbulence are predicted to be self-similar [3], i.e., the probability distribution function (PDF) for the difference between velocities measured at two points, $\delta v(\ell) = v(x + \ell) - v(x)$ (where v is along the line connecting the two points), should have a functional form independent of the separation ℓ . Self-similarity in a turbulent flow can also be determined from the scaling of structure functions, $S_p(\ell) \equiv \langle [\delta v(\ell)]^p \rangle \sim \ell^{\zeta_p}$: for any self-similar flow, ζ_p will vary linearly with p [1]. In particular, Kolmogorov's 1941 theory for homogeneous isotropic turbulence predicts the existence of an inertial range with $\zeta_p = \frac{p}{3}$.

Experiments and numerical simulations have shown that 3D turbulence is *not* self-similar [1]. The observed deviations from a linear dependence of ζ_p on p are attributed to the stretching and folding of vortices. As a vortex stretches, it shrinks in lateral extent until it collapses onto a singular line. Consequently, the energy dissipation rate varies with length scale. Vortex stretching is not allowed in 2D turbulence, and recent numerical simulations of 2D turbulence yielded self-similar behavior [4] (see also [3,5]). A recent experiment yielded self-similar behavior with a Gaussian PDF [6] while two other experiments showed scale-dependent statistics [7,8], as will be discussed later.

Our experiments on turbulent flow in a rapidly rotating annulus yield a self-similar PDF for the velocity differences, but the PDF is not Gaussian and the structure function exponent values ζ_p differ from the expected $p/3$. We now describe our experiments and then present the results.

Our apparatus consists of an annular tank filled with water and covered with a solid lid; the inner diameter of the tank is 21.6 cm and the outer diameter is 86.4 cm [10]. The depth of the tank increases from 17.1 cm at the inner radius to 20.3 cm at the outer radius [11]. Flow in the annulus is produced by continuously pumping water in a closed circuit through two concentric rings of 120 holes each in the bottom of the tank; the source ring is at a radius of 18.9 cm and the sink ring is at 35.1 cm. The radially outward flux from the pumping couples with the Coriolis force to generate a counter-rotating jet, which is wide and turbulent over a wide range of parameters. The rapid rotation leads to a flow that is essentially 2D except in the thin Ekman boundary layers at the top and bottom surfaces [10].

In the present experiments the tank rotates at 11.0 rad/s, sufficiently fast to produce an essentially 2D flow, and the flux is $150 \text{ cm}^3/\text{s}$, sufficiently large to produce an inverse energy cascade. The azimuthal velocity is measured using two hot film probes which are inserted through the top lid and extend 1 cm into the water on opposite sides of the tank, midway between the inner and outer walls. Each probe was sampled at 150 Hz for periods of two hours, giving 10^6 data points per probe for each run, and the measurements were repeated four times, yielding a total of 8×10^6 data points. Using the maximum velocity ($U_{max} = 22 \text{ cm/s}$) as the velocity scale and the distance between the forcing rings ($L = 16.2 \text{ cm}$) as the integral length scale, we calculate the Reynolds number to be 35,000 and the Rossby number ($U_{max}/2\Omega L$) to be 0.06.

Instantaneous 2D velocity fields were obtained using a Particle Image Velocimetry (PIV) system with a horizontal light sheet at mid-fluid depth and a rotating camera above the tank. For each flow condition, 50 instantaneous velocity fields were obtained, equivalent to approximately 2×10^5 velocity values at the radius of the hot film probes. Though this sample size is inadequate for high order statistics, the spatial information provided by the PIV measurements complements the long velocity time series obtained with the hot film probes. We also made PIV measurements at the same rotation rate at a higher pumping rate of $550 \text{ cm}^3/\text{s}$ ($Re = 100,000$).

Two vorticity profiles obtained with the PIV system are shown in Fig. 1. When the pump is first turned on, the flow consists of rings of cyclonic and anti-cyclonic vortices that form above the outlet and inlet rings, respectively. Vortices of like sign immediately begin merging and growing in size, and a counter-rotating jet forms between the two rings. At long times the inverse energy cascade leads to large vortices which are larger at higher pumping rates, as Fig. 1 illustrates.

We compute energy power spectra from the velocity time series data assuming Taylor's frozen turbulence hypothesis, which is applicable because the turbulent intensity (ratio of the rms velocity fluctuation to the mean velocity) is less than 10%. The spectra contain a region with $E(k) \sim k^{-2}$ (Fig. 2), in contrast with Kraichnan's prediction of $E(k) \sim k^{-5/3}$ for the inverse cascade [9]. Energy spectra obtained from PIV measurements of the azimuthal velocity data at $Re = 100,000$ show a scaling consistent with that obtained from the time series data, as shown in the upper curve of Fig. 2. A prediction of $E(k) \sim k^{-2}$ has been made for a turbulent flow made up of Lundgren spiral vortices that were not allowed to stretch in the third dimension [12]. Such scaling has also been predicted for rotating turbulent flows as they become 2D [13].

At high wavenumbers, our power spectra are consistent with those previously found for the forward (enstrophy) cascade, $E(k) \sim k^{-n}$, where $3 \leq n \leq 4$. However, our spectral range is too small to deduce a value for n .

By plotting the PDF for the velocity differences $\delta v(\ell)$ (Fig. 3), we obtain the first indication of self-similarity: data for different separations ℓ collapse onto a single curve when normalized. This curve is far from Gaussian, and the enhanced probability in the tails is likely due to the strong velocity differences that arise as coherent vortices pass the probes, as noted by She et al. [14].

Another indication of anomalous behavior is the scaling of the standard deviation of the velocity differences, δv_{rms} . Our data suggest $\delta v_{rms}(\ell) \sim \ell^{1/2}$ (see insets of Fig. 3) rather than the expected $\delta v_{rms}(\ell) \sim \ell^{1/3}$; the observed scaling of δv_{rms} is consistent with the scaling of

the energy spectrum in the inverse cascade range (Fig. 2).

Now we examine the structure function scaling, plotting S_p as a function of ℓ , as shown in Fig. 4(a). There is a scaling region (labeled A) from about 2 cm to 8 cm, and some indication of another scaling region (labeled B) for $\ell < 2$ cm; the transition between the two regions can be seen more clearly in the plot of $S_{10}/\ell^{5.5}$ vs. ℓ in the inset. The 2 cm lower limit of scaling of the structure functions is below the 5 cm ($k = 1.2 \text{ cm}^{-1}$ in Fig. 2) length where the energy spectrum behavior changes; this difference might be due to systematic error in calibration of the probes (note in Fig. 2 the difference in two probes at high wavenumbers), or perhaps because the scaling regions in real space and in Fourier space do not exactly correspond, as discussed in Ref. [1] (p. 62).

One test for the existence of an inverse energy cascade in 2D turbulence is the sign of $S_3(\ell)$: Kolmogorov's four-fifths law can be written for anisotropic flows as $\varepsilon = -\frac{1}{4}\nabla_\ell \cdot \langle |\delta\mathbf{v}(\ell)|^2 \delta\mathbf{v}(\ell) \rangle$, where \mathbf{v} is the full 3D velocity vector and ε is the mean rate of energy transfer (Ref. [1], p. 88). For the 3D forward cascade ε is positive; a negative value of ε corresponds to an inverse cascade. If the anisotropy is not too strong, the longitudinal S_3 dominates the transverse S_3 , and one can obtain the sign of ε from measurements of the longitudinal structure function alone. While our flows are anisotropic, we find that PDFs for velocity differences from PIV measurements in the radial and azimuthal direction are in agreement, indicating that the anisotropy does not strongly affect the velocity differences. The hot film data yield $S_3 > 0$ for $\ell < 10$ cm, which suggests that the inverse energy cascade stops at that point. This length corresponds visually to the scale of the largest vortices; thus region A corresponds to the inverse cascade. Scales below about 1 cm (the distance between the holes in the inner ring) presumably correspond to the forward enstrophy cascade.

The now standard way of extracting structure function exponents from data with limited inertial range is the technique introduced by Benzi et al. [15] called Extended Self-Similarity (ESS), where the ζ_p values are obtained from the slope of log-log plots of S_p vs. S_3 . The ESS plots of our data, Fig. 4(b), exhibit power law scaling through both ranges A and B, for lengths $0.5 < \ell < 15$ cm. Since S_3 should contain the same trends as the other structure functions, it is not surprising that the switching from region A to B is lost by this method.

The exponent values ζ_p deduced from the plot of $S_p(\ell)$ [region A in Fig. 4(a)] and from the ESS plot [Fig. 4(b)] are compared in Fig. 5. Region A of Fig. 4(a) yields $\zeta_{p,A} = p/2$, in contrast with theory, although $\zeta_{p,ESS} = p/3$, as it must for a self-similar flow.

Two recent experiments on turbulence in a quasi-2D fluid, a soap film, found departures from linear scaling of ζ_p vs. p [7,8], indicating that these flows were not self-similar. Another experiment on a quasi-2D flow, a magnetically driven shallow layer of electrolyte, yielded an inverse energy cascade with self-similar behavior as indicated by both the PDFs for δv and by the scaling of the structure function computed using ESS, which scaled as $\zeta_p = p/3$ [6]; however, the PDFs for δv were close to Gaussian, in contrast to those yielded by our flow (Fig. 3). A recent numerical simulation of 2D turbulence also yielded self-similar PDFs for δv , where the departure from Gaussianity, though small, contained significant information about the flow [4].

The $p/2$ scaling obtained for ζ_p in our flow may be a consequence of an inverse cascade driven by a radial velocity shear. This process would yield an energy flux $\varepsilon \sim \delta v_s (\delta v_\parallel)^2 / \ell$, where v_s would be a radial velocity due to the interaction of the vortices with the mean shear, v_\parallel the azimuthal velocity and ℓ the azimuthal separation. For a scale-invariant ε , the

resulting p^{th} order velocity structure function would have the scaling exponent $p/2$.

In summary, we find that turbulence in our rapidly rotating flow is self-similar, as indicated by the collapse of the PDFs onto a single curve and by the linear scaling of the structure function exponents. This self similarity extends over both the inverse and forward cascades. In the inverse cascade range, the flow exhibits anomalous scaling of the energy, $E(k) \sim k^{-2}$, and the structure functions, $S_p \sim \ell^{p/2}$, but this anomalous scaling is missed in an Extended Self Similarity analysis. We conclude that the rotation and strong shear make this flow different from 2D turbulent flows in non-rotating systems. Our results suggest that the transport and mixing in low Rossby number flows such as the atmosphere and oceans may be different from these processes in isotropic homogeneous 2D turbulent flows.

This research was supported by a grant from the Office of Naval Research. Z-S. S. acknowledges partial support from the Minister of Education in China and the Natural Science Foundation of China.

REFERENCES

- [1] U. Frisch, *Turbulence* (Cambridge University Press, 1995).
- [2] L.M. Smith and F. Waleffe, *Phys. Fluids* **11**, 1608 (1999).
- [3] E. D. Siggia and H. Aref, *Phys. Fluids* **24**, 171 (1981).
- [4] G. Boffetta, A. Celani, and M. Vergassola, *Phys. Rev. E* **61**, R29 (2000).
- [5] L. M. Smith and V. Yakhot, *Phys. Rev. Lett.* **71**, 352 (1993).
- [6] J. Parêt and P. Tabeling, *Phys. Fluids* **10**, 3126 (1998).
- [7] P. Vorobieff, M. Rivera, and R.E. Ecke, *Phys. Fluids* **11**, 2167 (1999).
- [8] W. B. Daniel and M. A. Rutgers, <http://www.arXiv.org/abs/nlin.CD/0005008> (2000).
- [9] R. H. Kraichnan, *Phys. Fluids* **10**, 1417 (1967).
- [10] T. H. Solomon, W. J. Holloway, and H. L. Swinney, *Phys. Fluids A* **5**, 1971 (1992).
- [11] The sloping bottom, a “beta plane”, approximates to first order the variation of the Coriolis force with latitude. The role of the beta plane, which breaks the symmetry between co-rotating and counter-rotating jets, will be the subject of a future study.
- [12] A. D. Gilbert. *J. Fluid Mech.* **193**, 475 (1988); *Phys. Fluids A* **5**, 2831 (1993).
- [13] Y. Zhou, *Phys. Fluids* **7**, 2092 (1995); V.M. Canuto and M.S. Dubovikov, *Phys. Rev. Lett.* **78**, 666 (1997).
- [14] Z.-S. She, E. Jackson, and S.A. Orszag, *Proc. Roy. Soc. London A* **434**, 101 (1991).
- [15] R. Benzi, S. Ciliberto, R. Tripicciono, C. Baudet, F. Massaioli, and S. Succi, *Phys. Rev. E* **48**, R29 (1993).

FIGURES

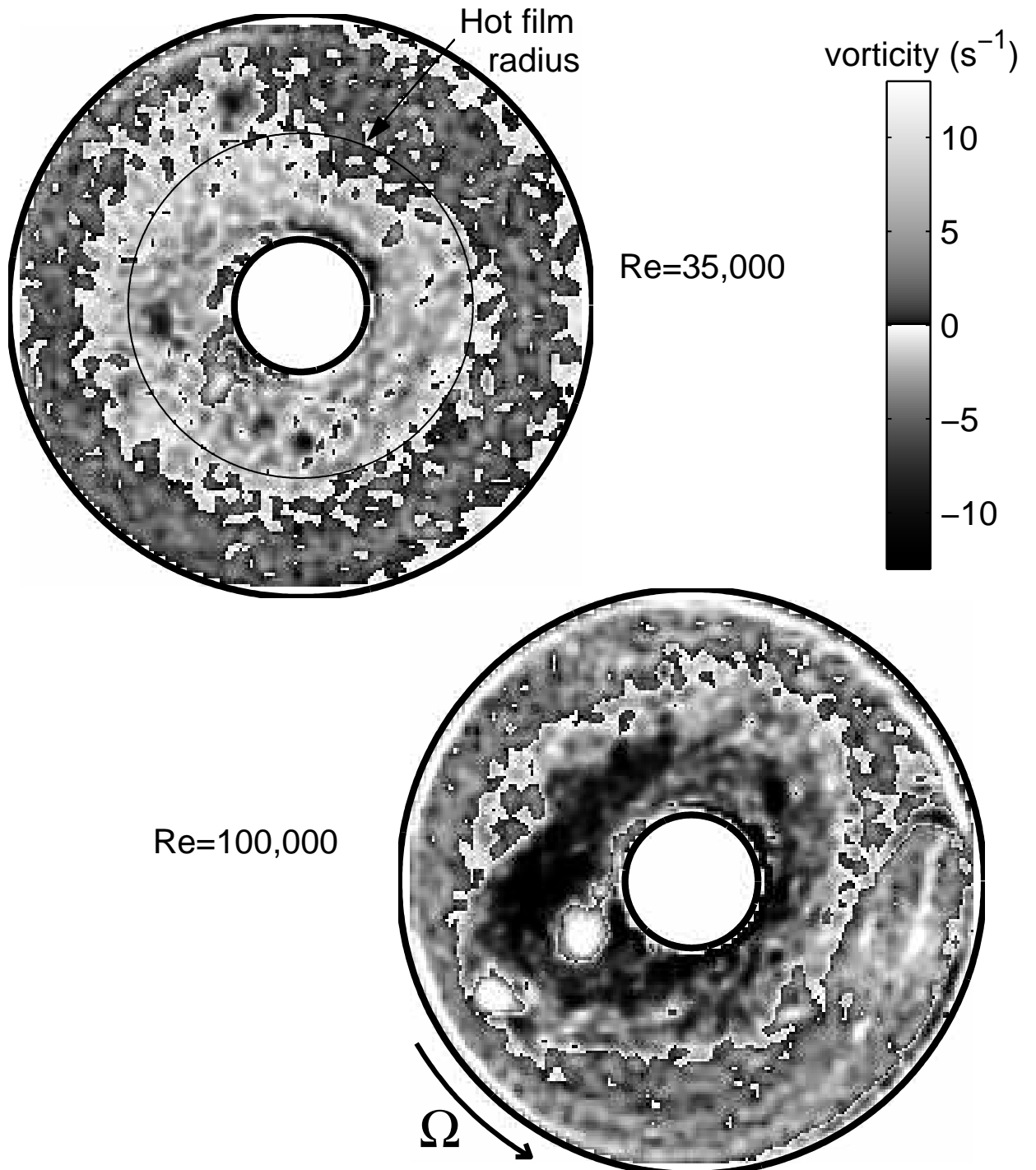


FIG. 1. Vorticity field at Reynolds number 35,000 ($Q = 150 \text{ cm}^3/\text{s}$) and 100,000 ($Q = 550 \text{ cm}^3/\text{s}$) for rotation rate 11.0 rad/s. Vortices with light (dark) center are cyclonic (anticyclonic). The vortices are advected by the clockwise jet.

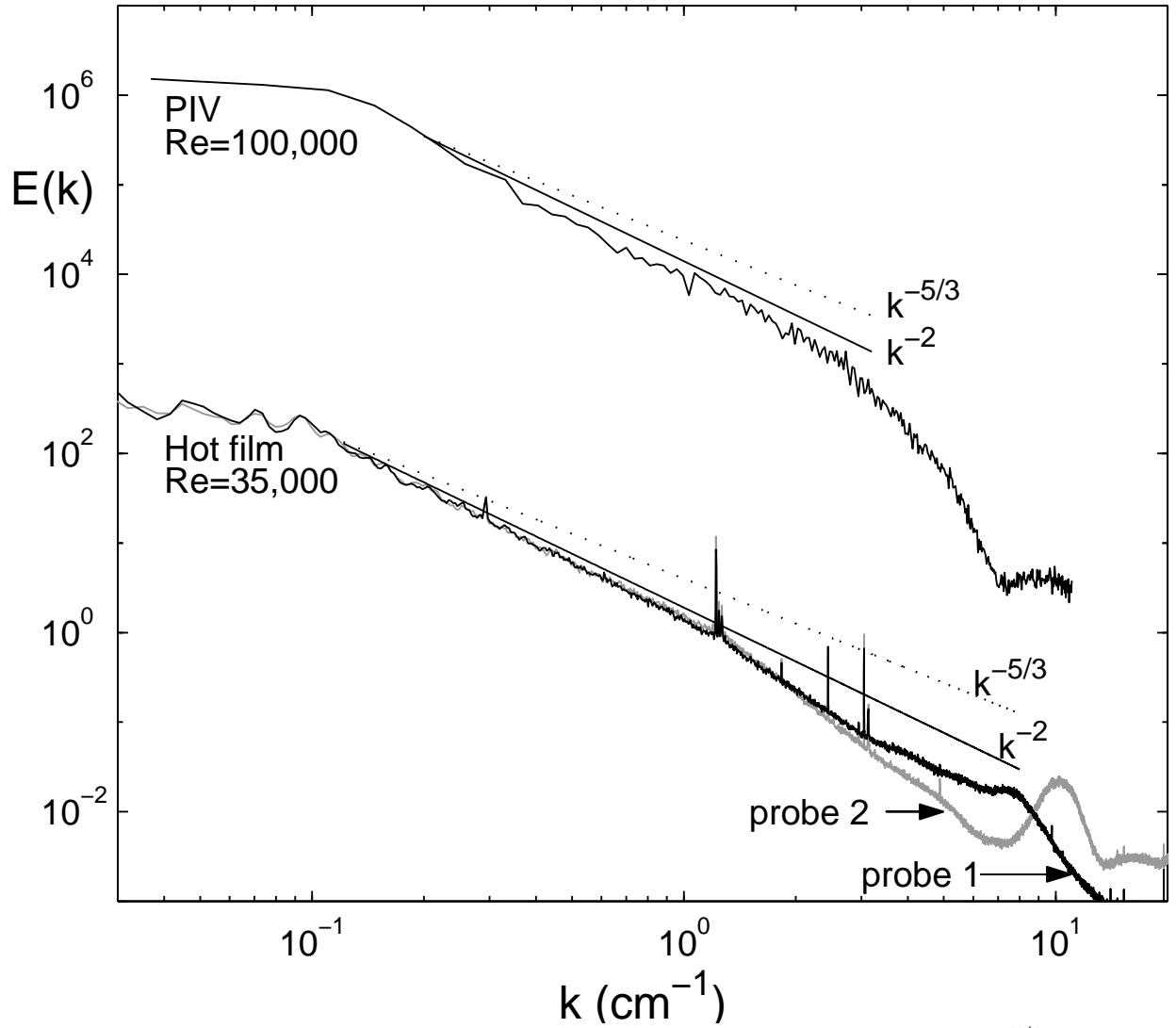


FIG. 2. Energy spectra (arb. units) with a dotted line showing the Kraichnan $k^{-5/3}$ inverse cascade and a solid line showing k^{-2} behavior. Fits of all of the hot film spectra in the range $0.1 < k < 1.22 \text{ cm}^{-1}$ give a slope of -2.04 ± 0.06 . The sharp spectral peaks correspond to harmonics of the tank's rotation rate, not to dynamics of the flow.

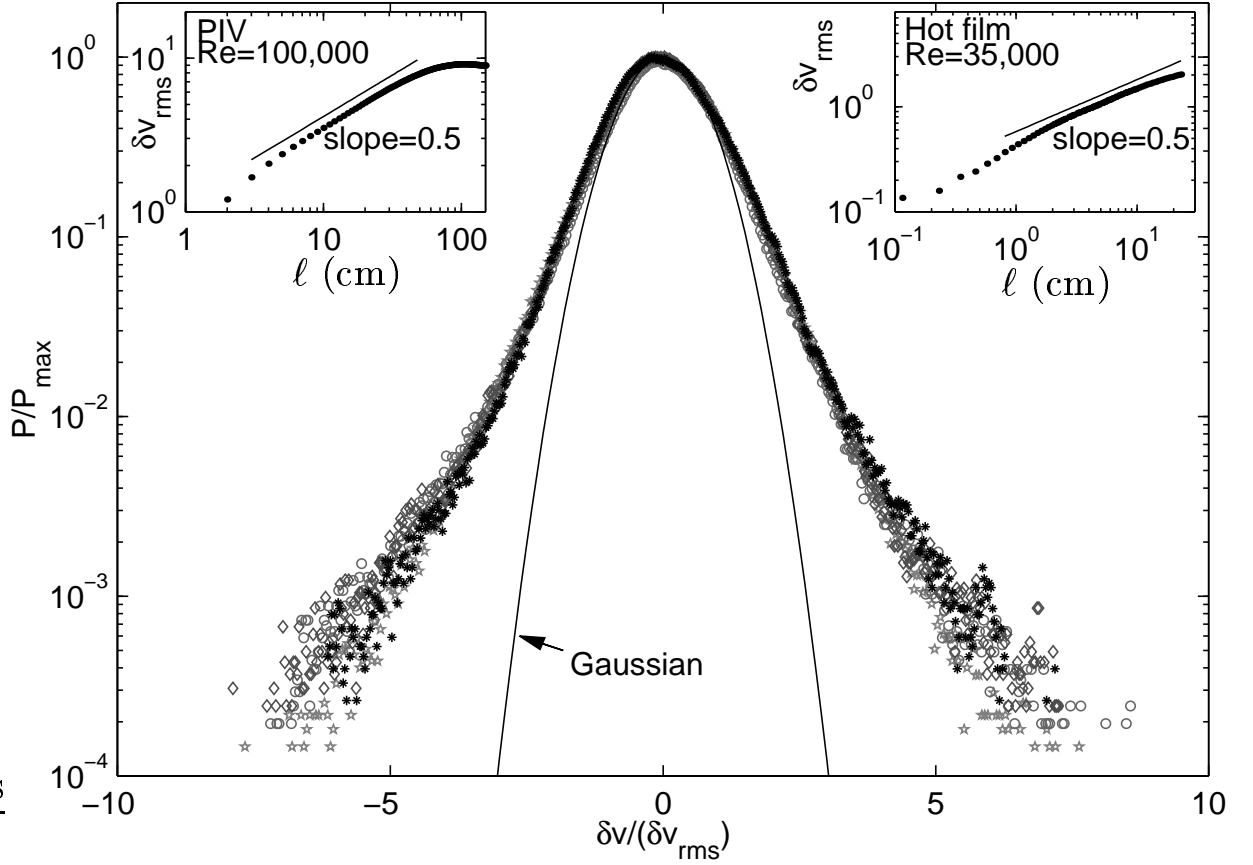


FIG. 3. Normalized probability distribution function for the velocity differences, demonstrating self-similar behavior: data for different separations ($l = 0.6, 4.6, 9.2, 17.3$ cm) collapse onto a single curve. The velocity differences are normalized by their standard deviation $(\delta v)_{\text{rms}}$ and the probability by its maximum value, P_{\max} . The standard deviation of the velocity differences (see insets) scales as l^α where $\alpha = 0.50 \pm 0.06$ for $Re = 35,000$ and $\alpha = 0.54 \pm 0.06$ for $Re = 100,000$.

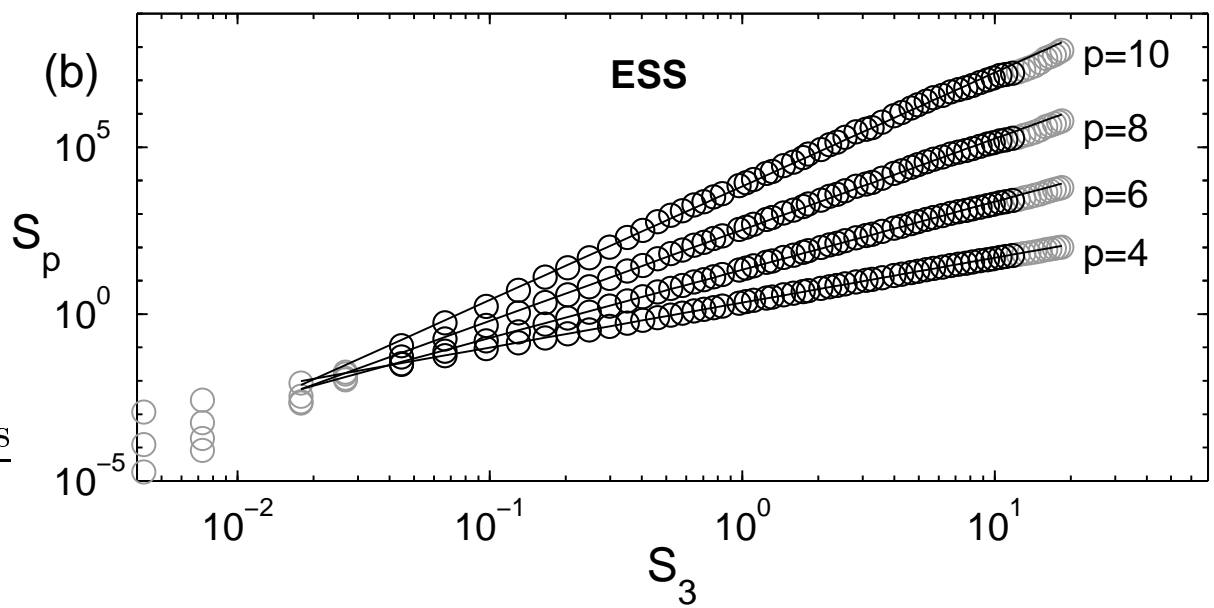
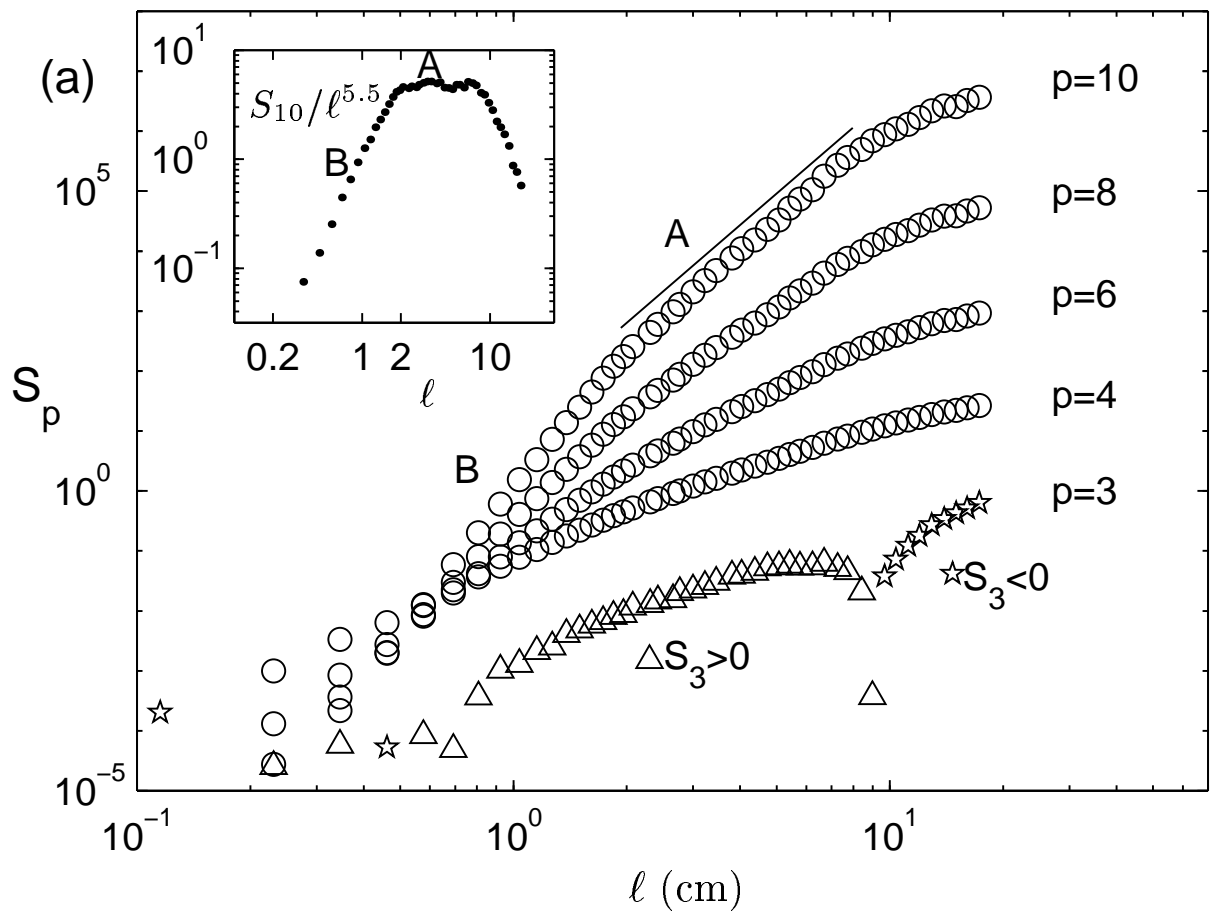


FIG. 4. Even order structure functions (a) as a function of ℓ and (b) as a function of S_3 (an Extended Self Similarity plot), for the hot film data at $Re = 35,000$. The graph of $S_{10}/\ell^{5.5}$ in the inset in (a) emphasizes the sharpness of the bend in S_{10} at $\ell \simeq 2$ cm. In (b) the dark symbols indicate the region from which the values of ζ_p were extracted.

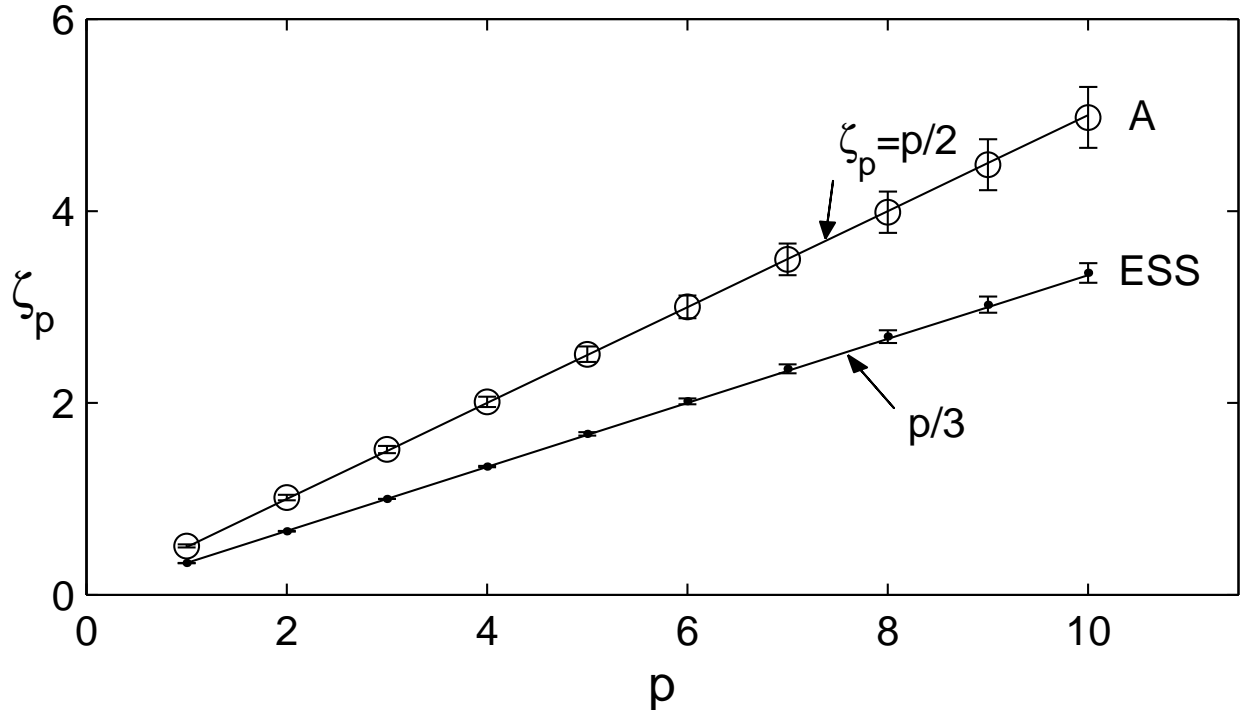


FIG. 5. Scaling exponents ζ_p as a function of p for region A of Fig. 4(a), and from the Extended Self Similarity analysis, Fig. 4(b). Region A, the inverse energy cascade region, yields $\zeta_p = (0.50 \pm 0.03)p$, while the ESS scaling shows the expected $\zeta_p = (0.33 \pm 0.01)p$ scaling over the forward and inverse cascade ranges. The error bars show the standard deviation of the eight separate data sets of 10^6 points.